Interpreting Imaging for Pre-Operative Planning and Execution of Glioma Surgery

Jun Muto, Zeya Aung Moe Thein, and Yuichi Hirose

1 Introduction

Glioblastomas are infiltrative brain tumors with poor prognoses despite multimodal treatment, and maximum safe resection is recommended whenever feasible. The extent of resection is positively correlated with survival [1].

The current standard for resection guidance is T2-weighted (T2W)-fluid attenuation inversion recovery magnetic resonance imaging (MRI) for non-enhancing gliomas and T1-weighted (T1W) MRI with a gadolinium-based contrast agent for enhancing gliomas.

The neurosurgeon's goal is to find the balance between maximizing the extent of resection and preserving brain function since surgery-induced neurological deficits result in lower quality of life and shorter duration of survival.

We have discussed the white fiber network, especially the superior longitudinal fasciculus (SLF) I, II, and III; arcuate fasciculus (AF); inferior frontooccipital fasciculus (IFOF); inferior longitudinal fasciculus (ILF); uncinate fasciculus (UF); cingulum; and corpus callosum (CC). Tractography requires that the region of interest (ROI)s are drawn over a specific fiber. And we also highlight how to set and draw the ROI for each essential white fiber.

This chapter reviews the understanding of the white matter network for each function and the course and radiographic findings for glioma surgery based on postmortem human brain dissection and tractography on MRI to aid pre-operative planning and surgical decision-making.

2 Case Presentation

2.1 Case 1

A 41-year-old male was referred to our hospital for headaches and vomiting that had lasted for 1 month. MRI of the brain with gadolinium administration showed a ring enhanced lesion in the right frontal lobe (Fig. 1a). The neuropsychological evaluation on admission revealed a severe headache. The rest of the neurologic examination findings were normal. The surgery involved a right frontotemporal approach to resect the tumor. Postoperative MRI demonstrated the total removal of the enhanced lesion (Fig. 1b). The essential related white fibers, in this case, were SLF I, II, and III; AF; and IFOF.

2.2 Case 2

An 81-year-old male presenting with headache and vomiting was brought to the emergency room.

J. Muto (✉) · Z. A. M. Thein · Y. Hirose
Department of Neurosurgery, Fujita Health University, Toyoake, Aichi, Japan
e-mail: muto@2002.jukuin.keio.ac.jp; muto@fujita-hu.ac.jp

A. Shah et al. (eds.), *Functional Anatomy of the Brain: A View from the Surgeon's Eye*,
https://doi.org/10.1007/978-981-99-3412-6_10

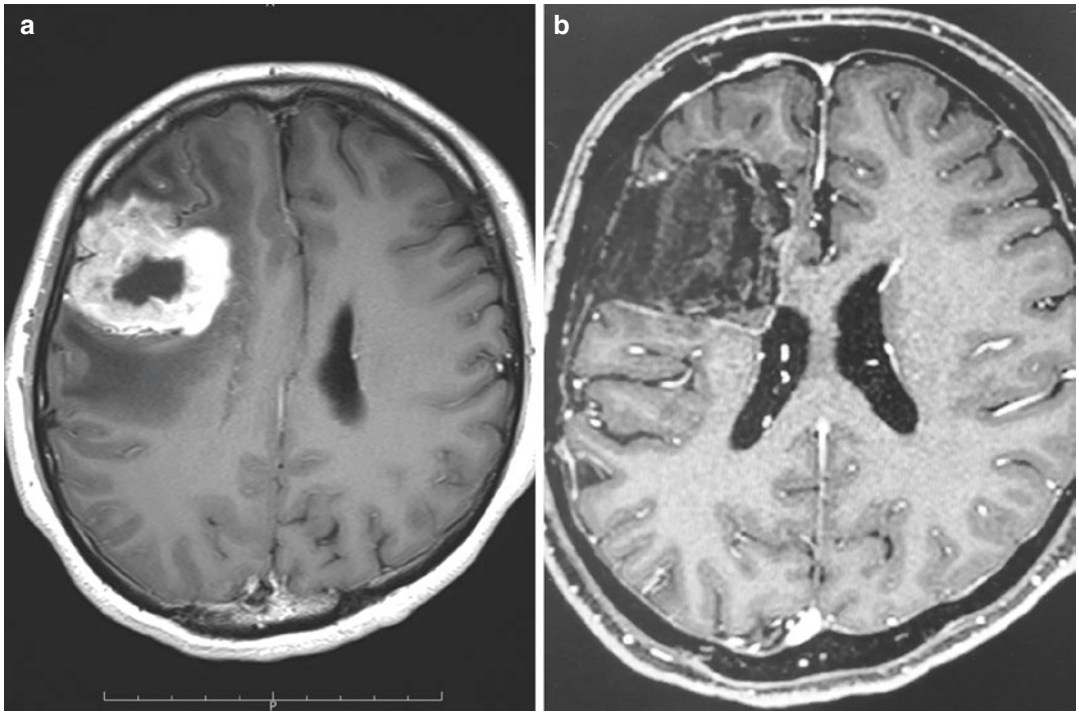

Fig. 1 Case 1 (**a**) A 41-year-old female with a ring-like enhanced lesion in the right frontal lobe on Gd-enhanced MRI before surgery. (**b**) Postoperative MRI showed complete removal of the enhanced lesion

MRI showed a ring enhanced lesion in the temporofrontal lobe with an extension to the parietal lobe with a high density on fluid attenuation inversion recovery MRI (Fig. 2a). The neuropsychological evaluation on admission revealed disorientation of time and place and difficulties with visual naming. The rest of the neurologic examination findings were normal. Surgery was performed, and a right frontotemporal approach was used to remove the enhanced lesion (Fig. 2b). The related essential white fibers were ILF, IFOF and UF.

2.3 Case 3

An 84-year-old female presenting with headache and vomiting was brought to the emergency room. MRI showed a ring-like enhanced lesion in the right parietal lobe (Fig. 3a). Surgery was performed, and a parietal transcortical approach was used to remove the tumor (Fig. 3b). The related white fibers were the cingulum, CC, corona radiata, and AF.

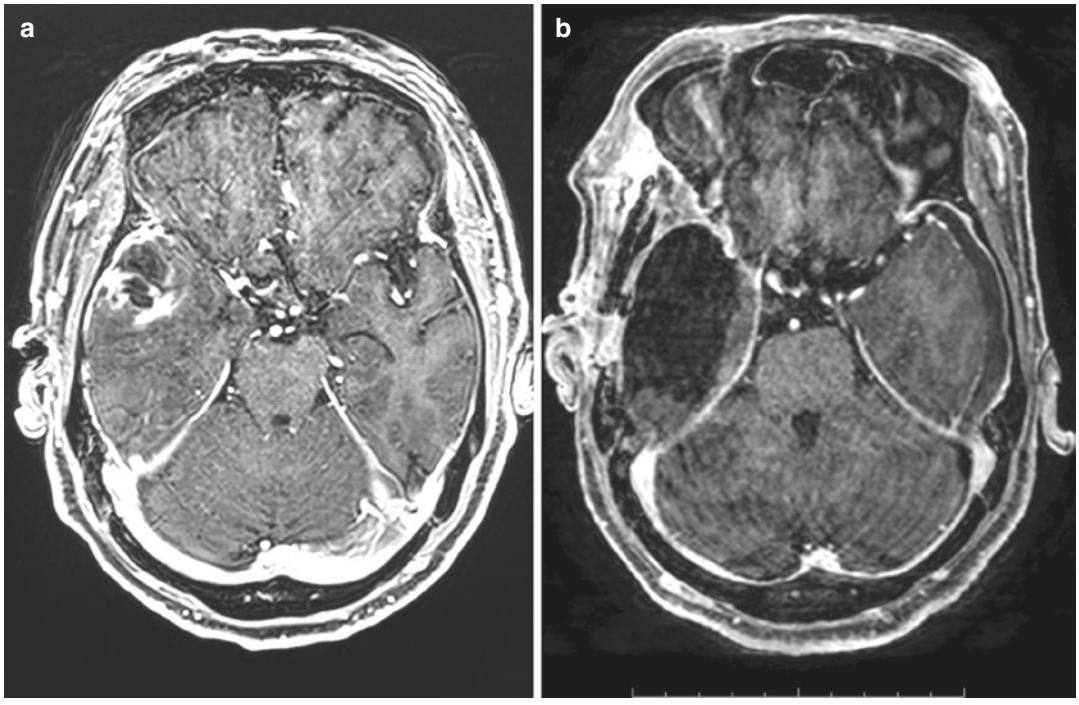

Fig. 2 Case 2. (**a**) An 81-year-old female with a ring-like enhanced lesion in the right temporal lobe on preoperative Gd-enhanced MRI. (**b**) Postoperative MRI showed complete removal of the enhanced lesion

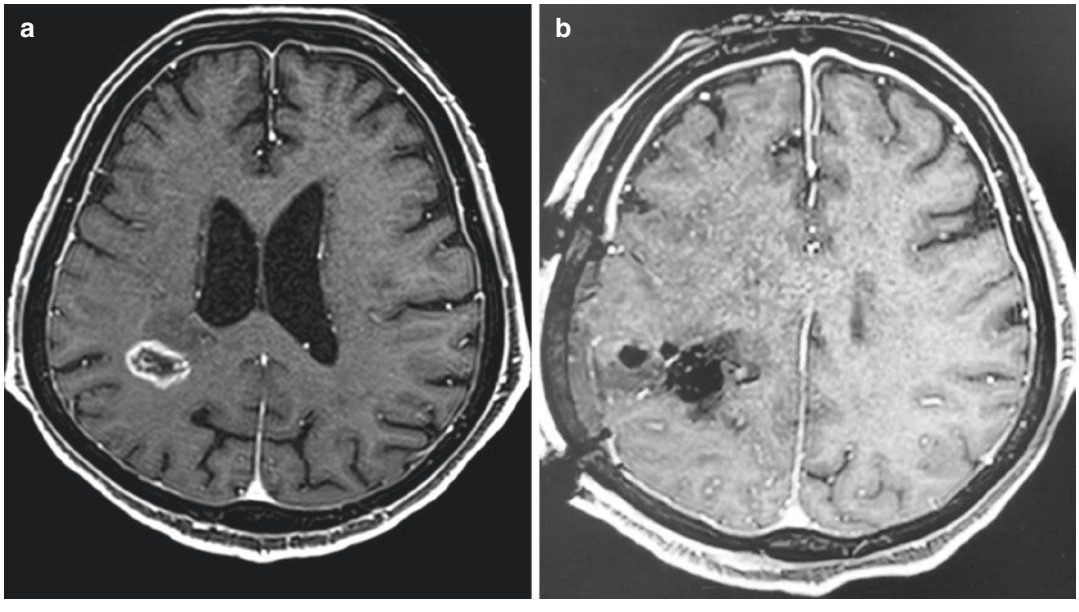

Fig. 3 Case 3. (**a**) An 84-year-old female with a ring-like enhanced lesion in the right parietal lobe on preoperative Gd-enhanced MRI. (**b**) Postoperative MRI showed complete removal of the enhanced lesion

3 White Matter Fibers

3.1 SLF I

The SLF I provides connections between the superior parietal lobe, which is important for recognizing limb and trunk locations in the body-centered coordinate space, and the premotor areas engaged in the higher aspects of motor behavior and the supplementary motor area, which is essential for intention and the initiation of motor activity. The SLF I runs from the precuneus (medial Brodmann area (BA) 7) and from the superior parietal lobule (BA 7) to the superior frontal gyrus (BA 8 and 9), supplementary motor area (BA 6), and anterior cingulate cortex, passing deep into the postcentral (BA 5) and precentral gyrus (BA 4). Therefore, the SLF I may be associated with higher-order control of body-centered action and the initiation of motor activity [2, 3].

On white-matter dissection, the SLF I is located within the medial part of the hemisphere and courses within the upper bank of the cingulate sulcus above the cingulum and medial to the callosal fibers. The cortex is above the cingulate sulcus, where the SLF I can be found.

During tractography, we reconstructed a system comprising three parallel longitudinal branches passing through the dorsolateral portion of the white matter situated above the ventricles and the lateral sulcus and connecting the parietal and the frontal lobes. The superior branch runs from the superior parietal lobule and the precuneus (BA7 and BA5) to the superior frontal gyrus (BA6, BA8, BA9 up to BA10). ROIs for the SLF I can be set within the suprafrontal gyrus (SLF1 I in green in Fig. 4a) and parietal lob (SLF I in green in Fig. 4b) in the coronal section and delete Tf in blue in Fig. 4c to allow the selection of the fiber running anteroposteriorly [4, 5] (Fig.4a–d).

3.2 SLF II

The SLF II is located within the middle part of the occipitoparietofrontal region, and it shows right dominance in 65% of the cerebral [6]. The SLF II extends from the occipital lobe (BA 19) and/or the upper part of the angular gyrus (BA 39) to the middle part of the middle frontal gyrus (dorsolateral prefrontal cortex; BA 46 and 9 or the lateral frontopolar cortex (BA10)) [7]. Functionally, the SLF II can regulate the focusing of attention on different parts of space because of its course, which connects the prefrontal cortex to the posterior parietal lobule. Likewise, damage to the SLF II is postulated to result in spatial working memory disorders such as neglect syndrome [2, 6].

Tractography shows that the middle branch connects the angular gyrus (BA39) to the posterior regions of the middle frontal gyrus (BA6) ventrally. Few projections continue further into the middle frontal gyrus up to BA46. ROIs for SLF II can be set within the middle frontal gyrus (SLF II in green in Fig. 4a) and parietal lobe (SLF II in green in Fig. 4b) in the coronal section and delete Tf in blue in Fig. 4c to allow the selection of the fiber running anteroposteriorly [5, 8] (Fig. 4a–c, e).

3.3 SLF III

The SLF III courses within the frontoparietal operculum and extends from the supramarginal gyrus (BA 40) to the pars opercularis (BA44) [6]. Functionally, the left SLF III is involved in phonological working memory, which is divided into a phonological store (in the left supramarginal gyrus) and an articulatory rehearsal module (in the left inferior frontal gyrus). Stimulation of the left SLF III produces articulatory disorders such as dysarthria or anarthria [9]. However, the right SLF III is involved in visuospatial attention, prosody, and music processing [6].

During white matter dissection, beginning from the level of the middle frontal gyrus, the cortex is removed to reveal the SLF. At first, the temporoparietal SLF (SLF-tp) can be exposed. It is recommended to preserve the white matter of the operculum, as the fibers of the SLF can easily be disrupted. SLF II can be located within the middle frontal gyrus with horizontal fibers and SLF III within the inferior frontal gyrus connect-

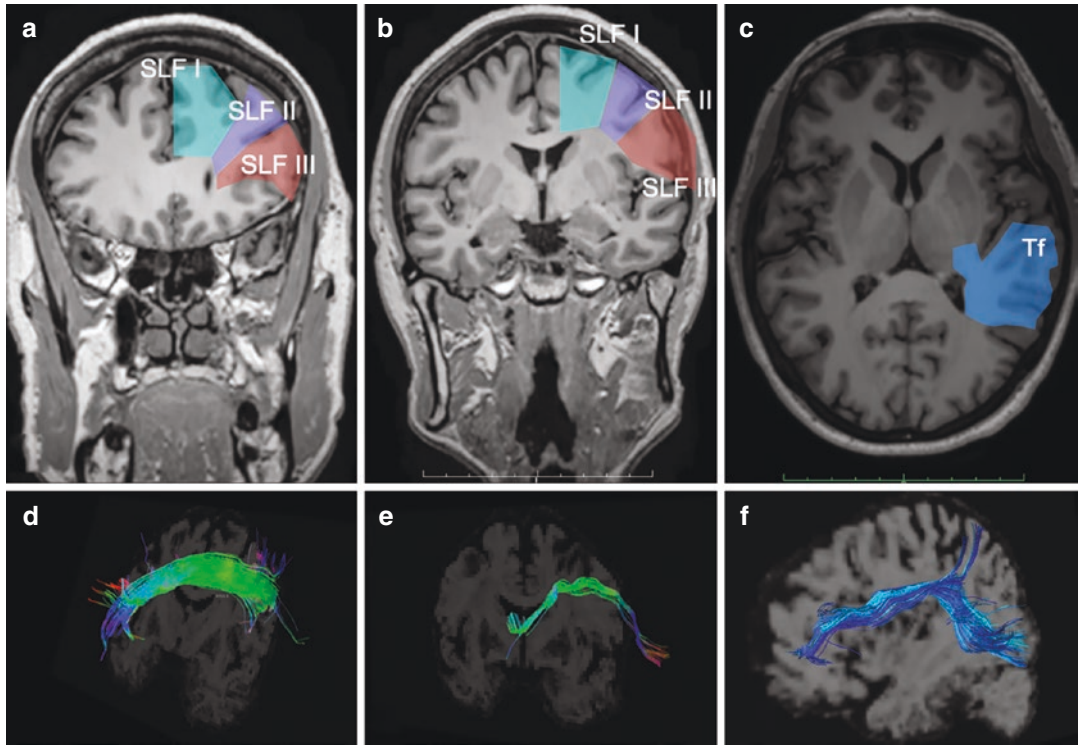

Fig. 4 Superior longitudinal fasciculis (SLF) I, II, and III. Delineation of the regions of interest (ROIs) used for tractography of the three subcomponents of parietofrontal connections. (**a**) Three ROIs in the left frontal lobe (SLF I, II, and III). (**b**) Parietal ROIs in the left hemispheres (SLF I in the superior frontal gyrus, SLF II in the middle frontal gyrus, SLF III in the inferior frontal gyrus). (**c**) Temporal ROI used to exclude the connections belonging to the temporofrontal arcuate fasciculus in the left (Tf) hemispheres. SLF I is the blue ROI in A and B, NOT Tf in C. SLF II is the purple ROI in (**a**) and (**b**), NOT Tf in C. SLF III is the red ROI in A and B, NOT Tf in (**c**). The multiple ROI approach was used to isolate the three components of the SLF (i.e. SLF I, SLF II, and SLF III). Three coronal ROIs were delineated around the white matter of the superior, middle, and inferior/precentral frontal gyri, and three other 'AND' ROIs were delineated posteriorly in the parietal region. Streamlines of the arcuate fasciculus projecting to the temporal lobe were excluded using an axial 'NOT' ROI in the temporal white matter (the arcuate is not part of the longitudinal system as it forms an arc to reach the temporal lobe). Tractography of SLF I (**d**), SLF II (**e**), and SLF III (**f**)

ing the supramarginal gyrus (BA 40) with the pars opercularis (BA44) (Figs. 6 and 7).

Tractography shows that the inferior branch originates in the supramarginal gyrus (BA40) and terminates in the pars opercularis (BA44), triangularis (BA45), and the inferior frontal gyrus (BA47) [8]. ROIs for the SLF III can be set within the inferior frontal gyrus (SLF III in green in Fig. 4a) and parietal lobe(SLF III in green in Fig. 4b) in the coronal section and delete Tf in blue in Fig. 4c to allow the selection of the fiber running anteroposteriorly [5, 8] (Fig.4a–c, f).

3.4 AF

The SLF and AF are the most superficial long association fibers visible after removing the cortex. The AF connects Broca's area, which is located within the frontal lobe, and Wernicke's area, which is located within the temporal lobe. The AF is divided into the ventral and dorsal segments based on its relationship with the supramarginal and angular parts of the inferior parietal lobe.

The AF ventral segment extends from the posterior (BA 22, BA 41, and BA 42) and the middle

parts (BA 21) of the middle temporal gyrus, passes deep into the lower part of the supramarginal gyrus (BA 40), and continues ventrally with the SLF III (ventral pathway) in the frontoparietal operculum to reach the pars opercularis (BA 44), triangularis (BA 45), and ventral premotor cortex (BA 6).

The AF dorsal segment extends from the posterior part of the middle (BA 37) and inferior (BA 20) temporal gyri, passes deep to the lower part of the angular gyrus (BA 39), and continues ventrally with the SLF II (middle pathway) to reach the pars opercularis (BA 44), ventral premotor cortex (BA 6), and posterior part of the middle frontal gyrus (BA 6) [7].

Functionally, the AF ventral segment is associated with phonological language processing in the dominant hemisphere, while the AF dorsal segment is associated with lexical and semantic language processing. In the inferior frontal cortex, cortical stimulation has been suggested to underlie separate language function subsystems for phonological (basic sounds that make up words), syntactic (principles and processes by which sentences are constructed), and semantic (concepts and meanings of words) processing. The phonological region is located posteriorly in the inferior frontal gyrus at the border of the pars triangularis (BA 45) and pars opercularis (BA 44). The semantic region is located anterosuperiorly in the inferior frontal gyrus and includes pars orbitalis (BA 47), triangularis (BA 45), and the dorsolateral prefrontal cortex (middle part of the middle frontal gyrus) (BA 46/9) [10]. In the nondominant hemisphere, the AF is involved in visuospatial processing [11] and some aspects of language such as prosody and semantics [12]. In the superior temporal cortex, functional studies suggest that the posterior part of the superior temporal gyrus (BA 22) is involved in phonological processing bilaterally, and the middle temporal gyrus (BA 21 and 37) is involved in lexical and semantic processing bilaterally, but prosody is exclusively processed in the right hemisphere [13].

During white matter dissection, the AF is a broad white matter tract that encircles the insula in the frontal, parietal, and temporal opercula. It connects the frontal, parietal, occipital, and temporal cortices and can readily be dissected [8] (Figs. 5, 6, and 7).

During tractography, the frontoparietal portion of the AF encompasses a group of fibers with anteroposterior directions running laterally to the projection fiber of the corona radiata. A single ROI (A) is used for the dissection of the AF. (A in

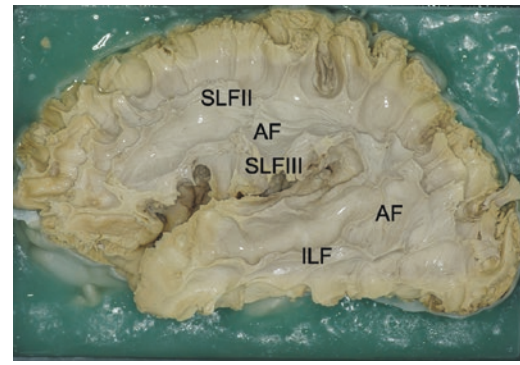

Fig. 5 Stepwise white matter dissection using the lateral approach. Dissecting the cortex from the frontal and temporal lobes. First, SLF-tp was identified in the temporoparietal lesion. SLF-tp originates posterior to the superior temporal gyrus and ascends to reach the superior parietal lobe. After removing SLF-tp, SLF II in the middle frontal gyrus, SLF III in the inferior frontal gyrus, AF around the perisylvian area, and ILF in the middle temporal gyrus can be observed. *AF* arcuate fasciculus, *ILF* Inferior longitudinal fasciculus, *SLF* Superior longitudinal fasciculus

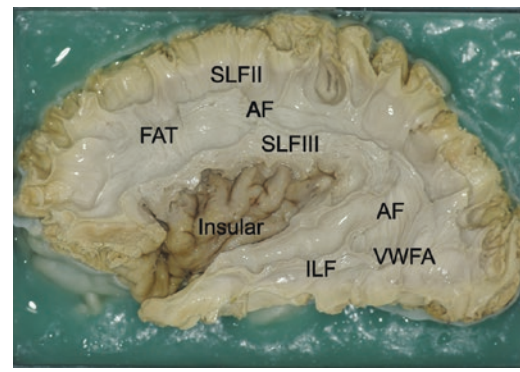

Fig. 6 Stepwise white matter dissection using the lateral approach. Removing the white matter of the operculum of the frontal and temporal lobes exposes the insula. Gradual dissection discloses the SLF more precisely. *AF* arcuate fasciculus, *FAT* Frontal aslant tract, *ILF* Inferior longitudinal fasciculus, *SLF* Superior longitudinal fasciculus, *VWFA* visual word forming area

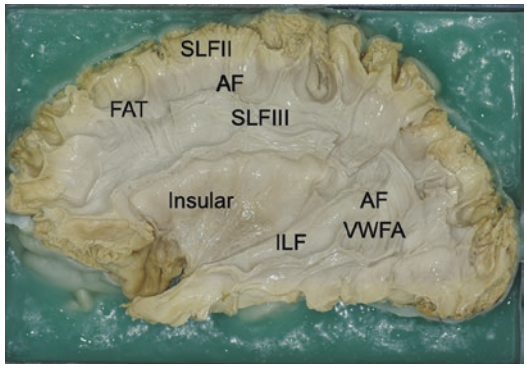

Fig. 7 Stepwise white matter dissection using the lateral approach. After acknowledging the insular surface anatomy and removing the gray matter of the insular, the fibers of the extreme capsule are exposed, and the gray matter of the claustrum can be observed. Removing the gray matter of the limen insular exposes the superficial layer of the uncinate fasciculus that is a part of the extreme capsule at this level. *AF* arcuate fasciculus, *FAT* Frontal aslant tract, *ILF* Inferior longitudinal fasciculus, *SLF* Superior longitudinal fasciculus, *VWFA* visual word forming area

Fig. 8a, b) A large half-moon-shaped region is delineated on the most dorsal part of the arcuate, usually one or two slices above the body of the CC. The lowest region is delineated around the posterior temporal stem. The medial border of the region is easy to identify from the FA maps as a black line between the arcuate and the corona radiata. The lateral border of the ROI passes through the bottom part of the frontal, parietal, and temporal sulci. The precentral sulcus demarcates the anterior border of the ROI, and the intraparietal sulcus is its posterior border [8] (Fig. 8a–c).

3.5 IFOF

Schmahmann and Pandya et al. [14] stated that the inferior occipitofrontal fasciculus corresponds to the extreme capsule, and the IFOF is one of the longest association fiber tracts of the

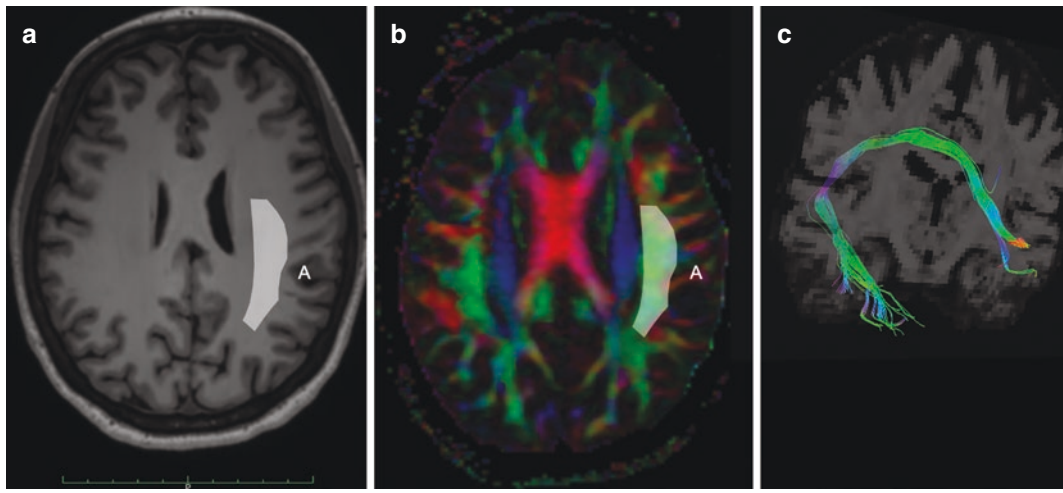

Fig. 8 AF. Delineation of the ROIs used for the tractography of the anterior and the long segments of the arcuate fasciculi. The frontoparietal portion of the arcuate fasciculus encompasses a group of fibers with anteroposterior directions (green) running laterally to the projection fiber of the corona radiata. A single ROI (**a**) is used for the dissection of the arcuate fasciculus in the T1-weighted image (**a**) and FA map (**b**). A large half-moon-shaped region is defined on the most dorsal part of the arcuate, usually one or two slices above the body of the corpus callosum. The lowest region is defined around the posterior temporal stem. The medial border of the region is easy to identify in the FA maps as a black line between the arcuate and the corona radiata. The lateral border of the ROI passes through the bottom part of the frontal, parietal, and temporal sulci. The precentral and intraparietal sulci demarcate the anterior and posterior borders of the ROI [4]. (**c**) tractography of right AF

brain. The IFOF may be split into superficial and deeper layers [15]. The superficial layer connects the frontal lobe to the superior parietal lobule and the posterosuperior part of the occipital lobe, whereas the deep layer connects the frontal lobe with the posteroinferior part of the occipital lobe and the posterobasal temporal areas.

Recent observations related to intraoperative stimulation during glioma surgery implicated the dominant ventral (anteroinferior) insular cortex in planning for motor speech [16, 17]. At the subcortical level, direct intraoperative stimulation of the ventral external (and extreme) capsule elicited paraphasic errors and repetition disorders characteristic of conductive aphasia [16, 18]. The inferior occipitofrontal fasciculus forms part of the ventral extreme and the external capsule and travels under the ventral insular cortex from the prefrontal to the posterotemporal regions. This fasciculus is the anatomic substrate of the ventral semantic pathway described by Duffau et al. [18] in contraposition to the dorsal phonological pathway. The IFOF is involved in reading [19], attention [11], and visual processing [20]. The IFOF may only exist in the human brain, and it is involved in verbal and visual semantic cognition [18, 21] and mentalizing [22].

During white matter dissection, the IFOF and UF can be observed beneath the limen insula after dissecting SLF I, II, II, AF, and the insular. The IFOF connects the frontal lobe to different territories of the posterior cortex. The extreme capsule is exposed when the anteroinferior portion of the insular cortex is removed. At the anteroinferior portion of the extreme and external capsules, the UF and the IFOF are exposed. In this region, both fasciculi narrow in section, and the IFOF is located dorsal and posterior to the UF. (Fig. 9).

During tractography, a two-ROI approach is used to dissect the fibers of the IFOF. The first region is delineated around the occipital lobe (O)) (Fig. 10a, b). The criteria used for the delineation of this occipital region have already been described in the paragraph of the ILF. The second region is delineated around the external/extreme capsule (E) (Fig. 10c, d), and the criteria for this delineation have already been explained in the paragraph of the UF [8]. (Fig. 10e, f).

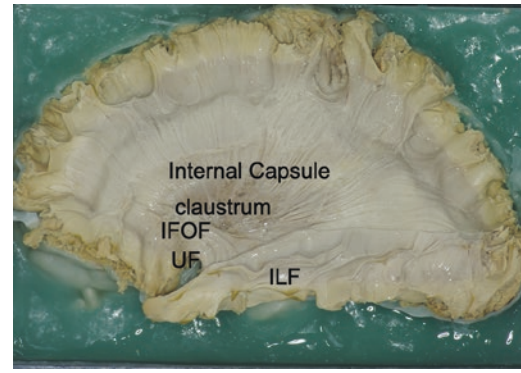

Fig. 9 Stepwise white matter dissection using the lateral approach. Dissecting the extreme capsule reveals the gray matter of the claustrum, whereas the IFOF and UF are revealed at the level of the limen insula. These white matter pathways are parts of the external capsule at the level of the limen insula. *AF* arcuate fasciculus, *IFOF* Inferior frontooccipital fasciculus, *ILF* Inferior longitudinal fasciculus, *UF* Uncinate fasciculus

3.6 ILF

The ILF connects the temporal pole with the dorsolateral occipital cortex and passes deep into the inferior temporal and inferior occipital gyri at the inferolateral edge of the temporal lobe. The ILF runs inferolateral to the temporal horn and atrium. The ILF in the right hemisphere forms a ventral occipitotemporal processing pathway with the IFOF, which is involved in visual identification and pattern discrimination, connecting regions of the core system of facial recognition; the fusiform gyrus seems to be especially important for processing facial identity [23, 24].The ILF in the left hemisphere forms the visual word form area (VWFA) at the crossing point of the posterior part of AF. VWFA is associated with alexia. Subcortical stimulation studies have demonstrated that (1) resection of the left ILFa does not induce alexia; (2) resection of the left ILFp leads to "pure alexia," namely alexia without aphasia

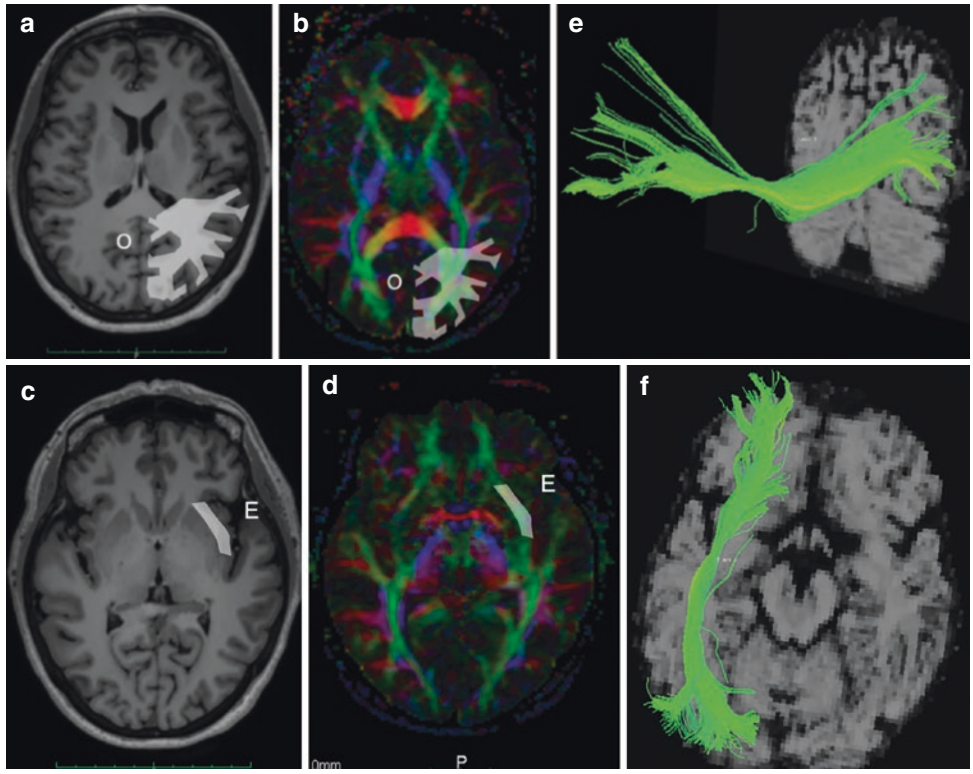

Fig. 10 IFOF. Delineation of the ROIs used for the tractography of the uncinate and the inferior frontooccipital fasciculus (IFOF). (**a**, **b**) Occipital lobe (O) in the hemispheres on the T1-weighted image (**a**) and FA map (**b**). (**c**, **d**) External/Extreme capsule ROIs (e) in the hemisphere on the T1-weighted image (**c**) and FA map (**d**). A two-ROI approach (O) AND (**e**) was used to isolate the inferior frontooccipital fasciculus. (**e**, **f**) tractography of IFOF

and agraphia, by disconnecting the VWFA from its main visual inputs; (3) the most anterior part of the VWFA is required to allow "addressed phonology" through the lexical-semantic pathway, i.e., to read irregular words; and (4) inferior termination of the AFp in the ITGp is a crucial part of the network involved in assembled phonology and in reading pseudowords and irregular words aloud [25]. The ILF is involved in facial recognition [26], visual perception [27], reading [19], visual memory [28], and other functions related to language [8].

During white matter dissection, removing the vertical part of the SLF exposes a group of horizontal fibers (such as the sagittal stratum) situated within the posterior temporal and occipital areas. This compact bundle comprises the fibers of the inferior occipitofrontal fasciculus, anterior commissure, ILF. The gray matter of the insula can be peeled away until its connective fibers, which constitute the superficial layer of the extreme capsule, are evident. Removing the gray matter of the limen insula, in particular, exposes the superficial layer of the UF, which is essentially a part of the extreme capsule at this level. Dissecting the extreme capsule reveals the ventral part of the external capsule. The claustrum becomes apparent at the level of the insular apex, whereas the occipitofrontal and uncinate fasciculi are depicted at the level of the limen insula [29]. (Figs. 5, 6, 7, and 9).

During tractography, a two-ROI approach is used to dissect the ILF. The first ROI (T in Fig. 11a, b)is delineated around the white matter

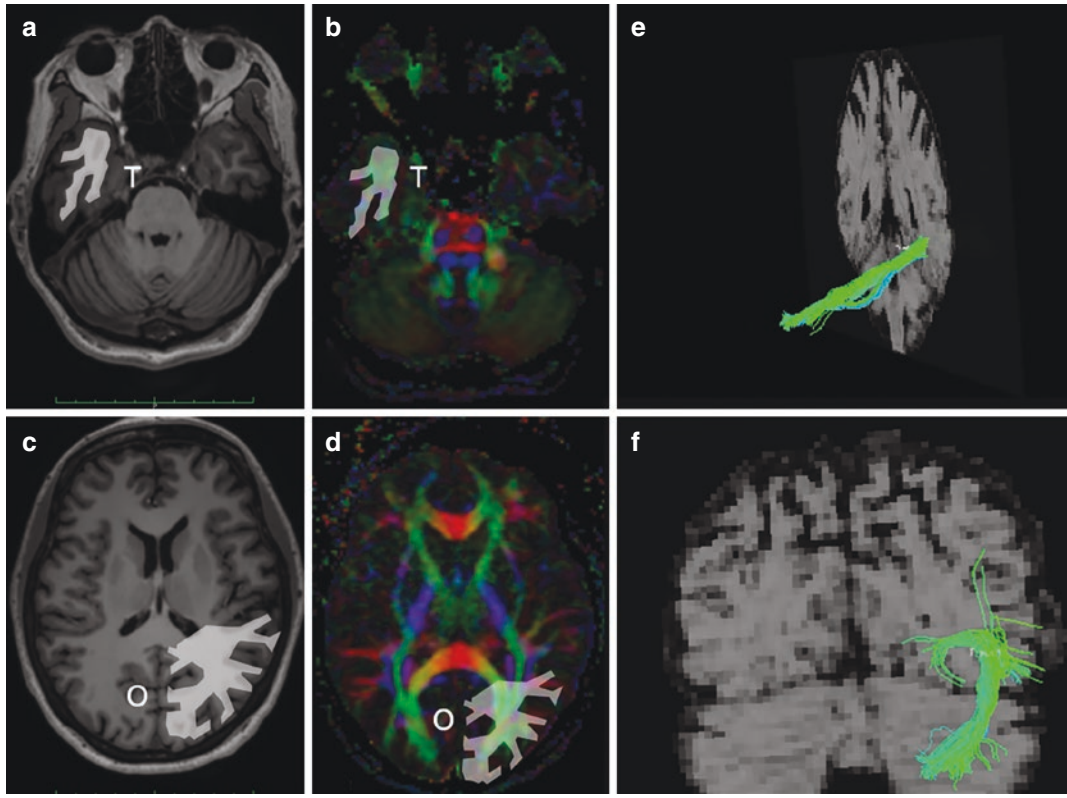

Fig. 11 ILF. Delineation of the ROIs used for the tractography of the inferofrontal longitudinal fasciculus. (**a**, **b**) Temporal lobe ROI (T) in the hemispheres on T1-weighted image (**a**) and FA map (**b**). (**c**, **d**) Occipital lobe ROI (O) in the hemisphere on a T1-weighted image (**c**) and FA map (**d**). A two-ROI approach was employed to isolate the inferior frontal longitudinal fasciculus. For each hemisphere, we delineated an axial ROI (T) AND (O). (**e**, **f**) tractography of ILF

of the anterior temporal lobe. The first region of the temporal ROI is delineated on a slice located three slices below the slice containing the junction between the frontal and temporal branches of the anterior floor of the external capsule. It is important to exclude the most posterior white matter of the temporal lobe to prevent contamination from fibers belonging to other tracts. The second ROI (O in Fig. 11c, d) is delineated around the white matter of the occipital lobe. The anterior border should always be posterior to the tip of the occipital horn or cingulum [4]. (Fig. 11e, f).

3.7 UF

The UF is a bidirectional long-range white matter tract that connects the lateral orbitofrontal cortex and BA 10 with the anterior temporal lobes.

Abnormalities in the UF have been associated with several psychiatric disorders, and previous studies have suggested that it plays an important role in episodic memory, language, and social-emotional processing; however, its exact function is not well-understood.

Von Der Heide RJ et al. proposed that the role of the UF is to allow temporal lobe-based mnemonic associations, such as an individual's name + face + voice, to modify behavior through interactions with the lateral orbitofrontal cortex, which provides valence-based biasing of decisions. The bidirectionality of the UF information flow allows orbital and frontal cortex-based reward and punishment history to rapidly modulate temporal lobe-based mnemonic representations. UF is involved in emotion processing, memory [28, 30]. and language functions [8]. The disruption of the uncinate may cause problems in the expression of memory to guide deci-

sions and the acquisition of certain types of learning and memory. Moreover, uncinate perturbation should cause problems that extend beyond memory to include social and emotional problems due to people and objects being stripped of personal value and emotional history and lacking in higher-level motivational value [31]. During white matter dissection, the UF can be found after removing the gray matter of the insular and the limen insular, which is essentially a part of the extreme capsule at this level. Superficially, the extreme capsule, claustrum in gray matter, external capsule, putamen in gray matter, and the internal capsule can be found individually. After dissecting the putamen, which has a spongy consistency, the firm density of the globus pallidus is identified. The occipital frontal and UF are left in place. (Fig. 9).

During tractography, a two-ROI approach is used to dissect the UF. The first ROI (temporal, T) (Fig. 12a, b) is placed within the anterior temporal lobe, as described for the ILF. A second ROI (external/extreme capsule, E) (Fig. 12c, d) is delineated around the white matter of the anterior floor of the external/extreme capsule. The insula delineates the lateral border of the ROI, with the lenticular nucleus as its medial border. We suggest beginning the delineation of this second ROI from the slice where the temporal and frontal branches of the external/extreme capsule join (Fig. 12e, f).

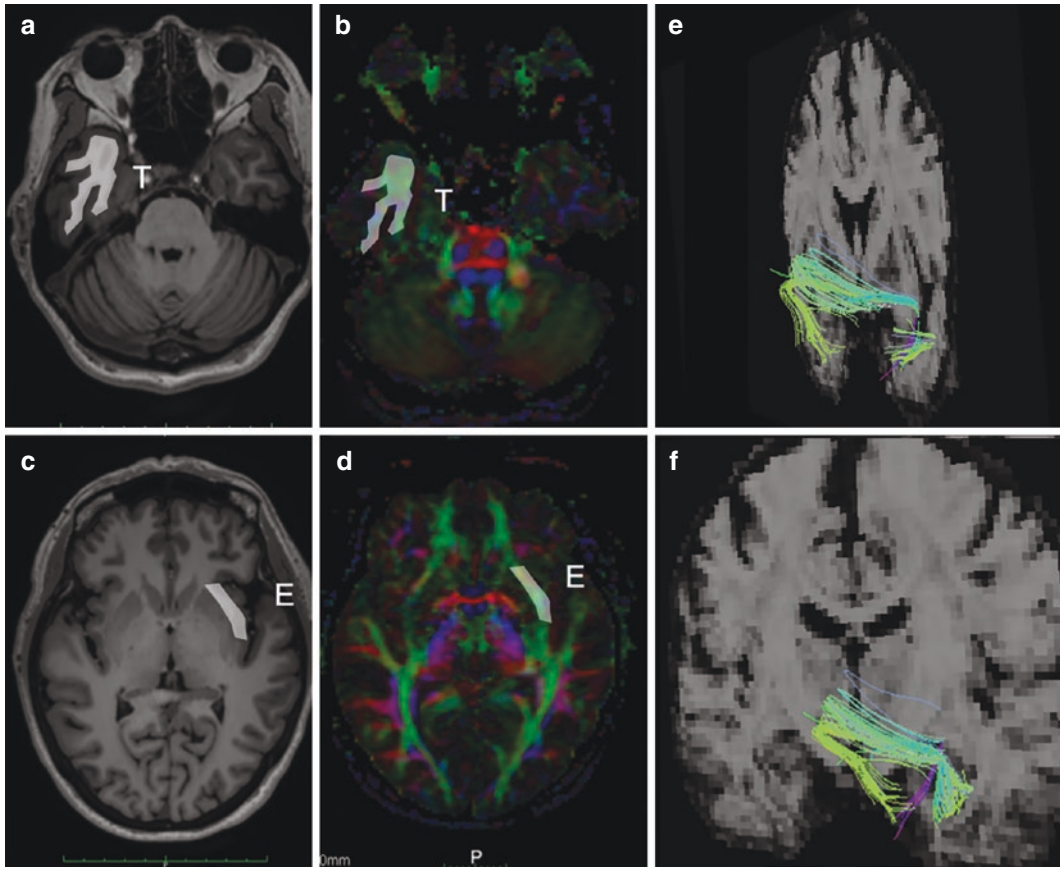

Fig. 12 UF. Delineation of the ROIs used for the tractography of the uncinate fasciculus. (**a**, **b**) Temporal lobe ROI (T) in the hemispheres on T1-weighted image (**a**) and FA map (**b**). (**c**, **d**) External/Extreme capsule ROIs (**e**) in the hemisphere on a T1-weighted image (**c**) and FA map (**d**). A two-ROI approach was employed to isolate the inferior frontal longitudinal fasciculus. For each hemisphere, we delineated an axial ROI (T) AND (E). (**e**, **f**) tractography of UF

3.8 CC

The CC is the largest white matter structure in the brain, consisting of 200–250 million contralateral axonal projections and the major commissural pathway connecting the hemispheres of the human brain. Four named regions are described by anatomists for the CC. These are, from the anterior to the posterior, the rostrum, the genu, the body, and the splenium [32]. While this classification is still widely used today, it does not define the boundaries between the different segments. A second tentatively better parcellation was based on histological measures of the midsagittal axonal diameter but it could not be systematically generalized across individuals [33]. The enforcement of a geometrical grid of seven parcels has been used to somewhat circumvent the limitations of generalization [34]. All these anatomical, histological, and geometrical parcellations of the midsection of the CC do, however, not consider the functional organization of the brain areas it connects.

Since the functions of the CC are defined by the areas that it connects to, tract-tracing in nonhuman primates or diffusion-weighted imaging tractography in humans is likely the most promising approach to investigate the functional organization of the CC. Friedrich et al [35] provided the first comprehensive map of the callosal cross-section that displays the distribution of callosal connections according to a hierarchical organization of cognitive functions without enforced boundaries [35].

During white matter dissection, the CC is on the medial side. The gray matter of the medial cerebral surface should be peeled away starting from the depth of the anterior part of the cingulate sulcus [36]. Subsequently, the CC can be resected, leaving a thin strip attached to the cingulum. The "U" fibers and the white matter of the superior arm of the cingulum should be dissected to reveal the radiating fibers of the CC.

During tractography, a single ROI (CC) (Fig. 13a, b) is delineated around the body, the genu, and the splenium of the CC. The shape of the regions follows the anatomy of the different parts of the CC: butterfly shape for the body and horseshoe shape for the genu and splenium. Alternatively, a single ROI delineated around the CC on a midsagittal slice can be used (Fig. 13c, d).

3.9 Cingulum

The cingulum is part of the limbic system and is involved in attention, memory, and emotions [20].

The cingulum bundle (CB) forms connections between the frontal lobe, parietal lobe, and temporal lobe, which are associated with cognitive and emotional processing implicated in the pathophysiology of numerous psychiatric disorders. CB-I ran from the subrostral areas to the precuneus and splenium, encircling the CC. CB-II arched around the splenium and extended anteriorly above the CC to the medial aspect of the superior frontal gyrus (SFG). CB-III connected the superior parietal lobule (SPL) and precuneus with the medial aspect of the SFG. CB-IV was a relatively minor subcomponent from the SPL and precuneus to the frontal region. CB-V, the parahippocampal cingulum, stemmed from the medial temporal lobe and fanned out to the occipital lobes [37]. CB-V supposedly participates as a major subcortical stream within the default mode network, possibly subserving the transfer of multimodal cues relevant to visuospatial, facial, and mnemonic information to the precuneal hub [38].

During white matter dissection, the cingulum is observed on the medial side [39, 40]. The gray matter of the medial cerebral surface should be peeled away, starting from the depth of the anterior part of the cingulate sulcus and gradually extending posteriorly to the precuneus. Attention should be paid to the dissection of the cingulum, as it is easily disrupted, especially in its inferior arm such as the parahippocampal gyrus.

During tractography, a single ROI (Ci) (Fig. 14a, b) is used to dissect the cingulum. A single cigar-shaped region is defined on the top three slices. When the cingulum separates into two branches, an anterior and posterior region is

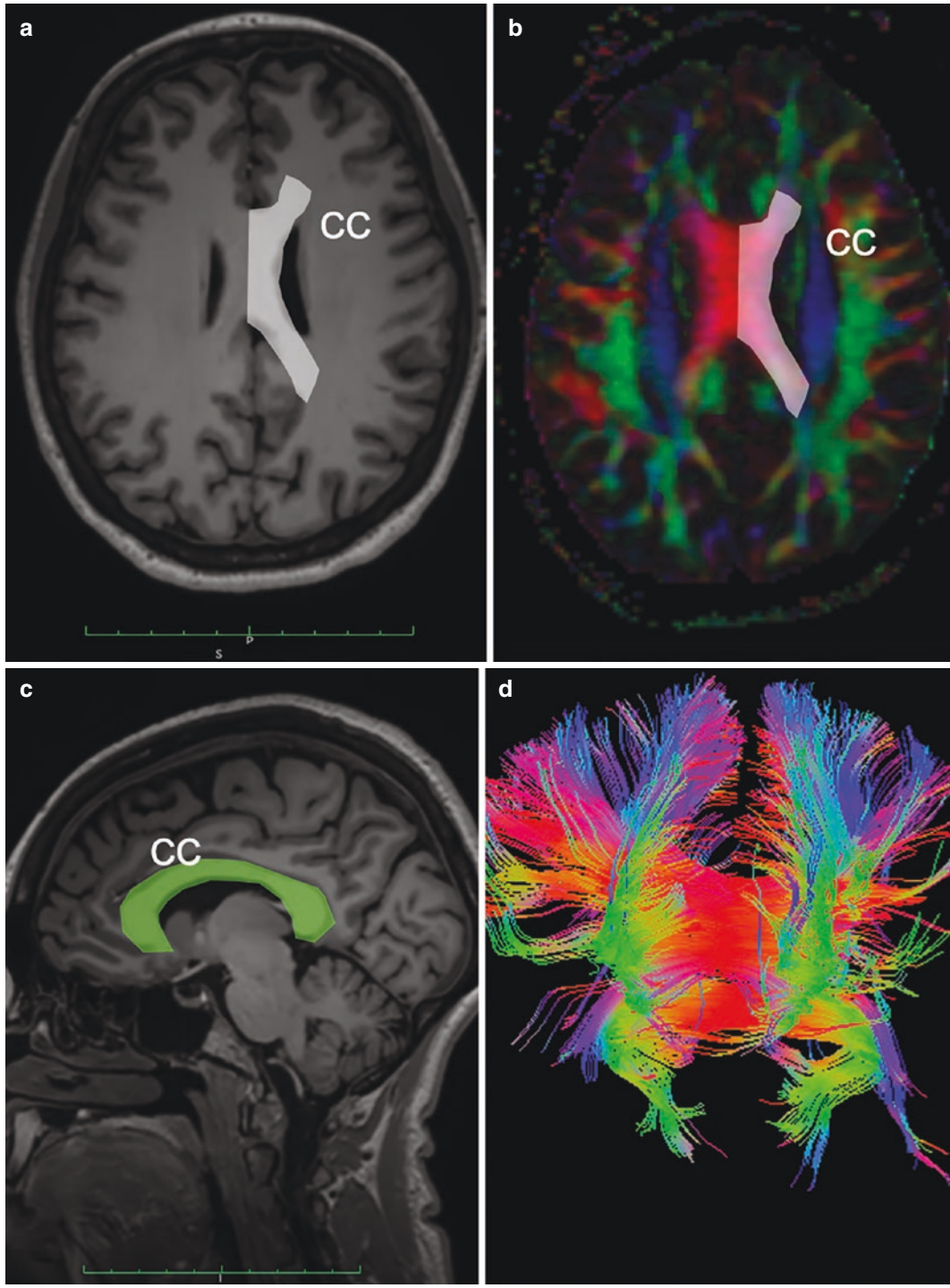

Fig. 13 Corpus callosum. Delineation of the ROI: A single ROI (CC) is delineated around the body, the genu, and the splenium of the corpus callosum on the T1-weighted image (**a**) and FA map (**b**). The shapes of the regions follow the anatomy of the different parts of the corpus callosum: butterfly shape for the body and horseshoe shape for the genu and splenium. (**c**) Alternatively, a single ROI around the corpus callosum on a midsagittal slice can be used. (**d**) tractography of the Corpus callosum

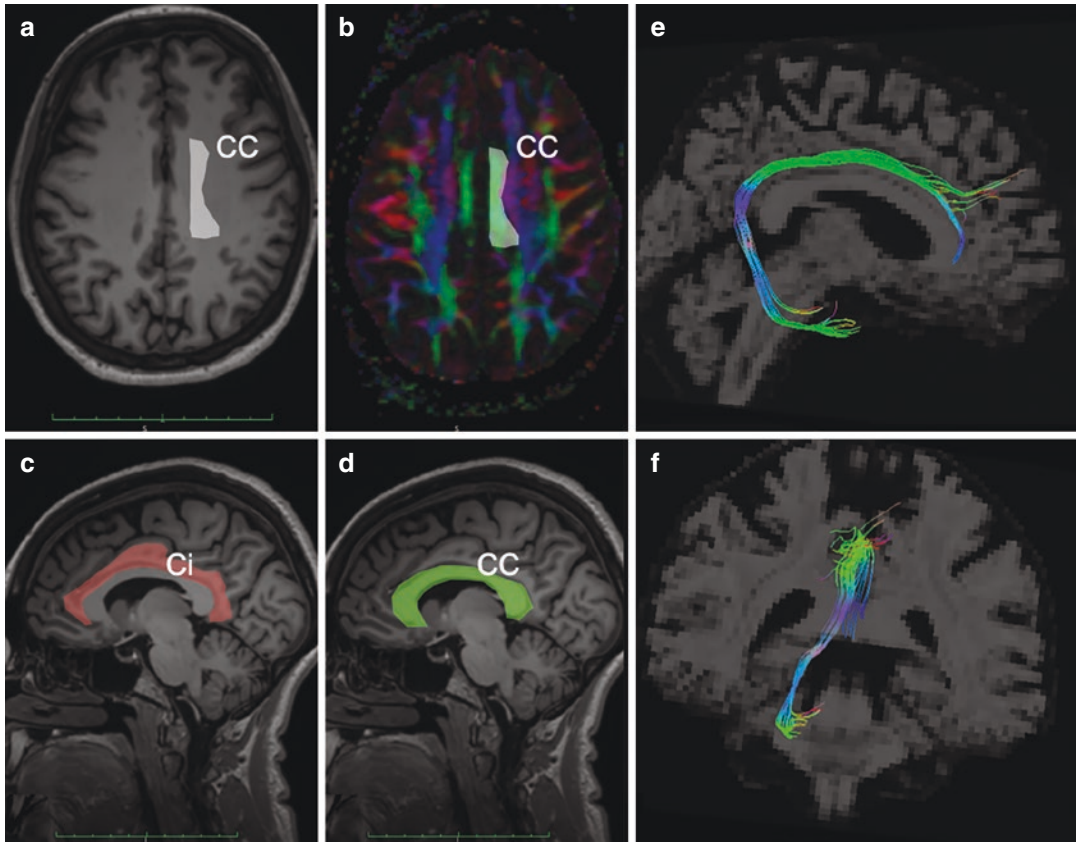

Fig. 14 Cingulum. Delineation of the ROIs used for tractography of the cingulum. A single ROI (Ci) is used to dissect the cingulum. A single cigar-shaped region is delineated in an axial slice on the T1 weighted image (**a**) and FA map (**b**). It is important to remember that the majority of the fibers of the cingulum are short U-shaped fibers connecting adjacent gyri. The use of a two-ROI approach excludes the majority of these short fibers from the analysis. (**c**) Cingulum ROI (Ci) in the hemisphere. (**d**) Corpus callosum ROI (CC) in the medial section to exclude the connections belonging to the corpus callosum. A two-ROI approach was used to isolate the cingulum fasciculus (**c**) NOT (**d**). A sagittal ROI was set around the white matter of the cingulum for the hemispheres. Streamlines of the corpus callosum projecting to the hemisphere opposite to the ROI were excluded using a sagittal 'NOT' ROI on the corpus callosum. (**e**, **f**) tractography of the Cingulum

delineated on each slice. It is important to remember that the majority of the fibers of the cingulum are short U-shaped fibers connecting the adjacent gyrus. The use of a two-ROI approach excludes the majority of these short fibers from the analysis. For this reason, the use of the one-ROI approach ROI (Ci) (Fig. 14a, b) or ROI Ci (Fig. 14c) without fibers of ROI CC (Fig. 14d), which includes all fibers of the cingulum is recommended (Figs. 14e, f, 15, and 16).

Ethical Approval All procedures performed in this study involving human participants were in accordance with the ethical standards, of the institutional research committee of the hospital of Fujita Health University with the 1964 Helsinki declaration and its later amendments or comparable ethical standards.

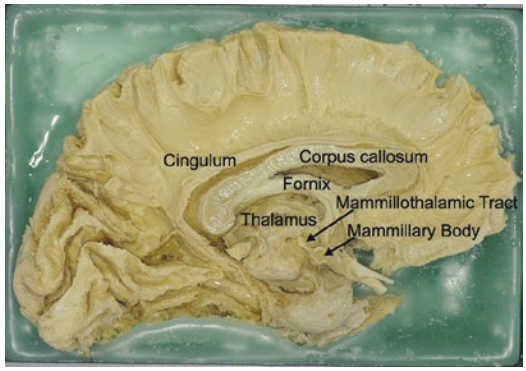

Fig. 15 Stepwise white matter dissection using the medial approach. The gray matter of the medial cerebral surface should be peeled away. Attention must be given to the dissection of the cingulum, as it is easily disrupted, especially in the inferior arm of the parahippocampal gyri. Subsequently, the cingulum fibers will be exposed

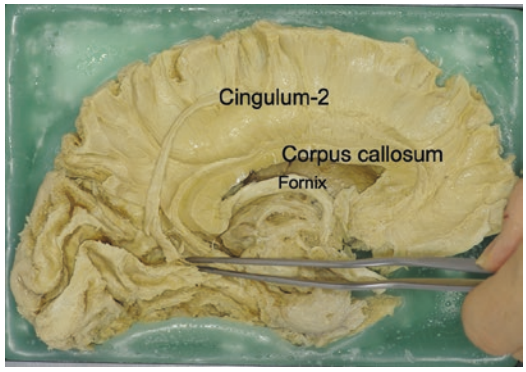

Fig. 16 Stepwise white matter dissection using the medial approach. The cingulum fibers consist of five layers. The CB2 (the second part of the cingulum) was held by the forceps

References

1. Sanai N, Polley MY, McDermott MW, Parsa AT, Berger MS. An extent of resection threshold for newly diagnosed glioblastomas. J Neurosurg. 2011;115(1):3–8. https://doi.org/10.3171/2011.2.JNS10998.
2. Makris N, Kennedy DN, McInerney S, et al. Segmentation of subcomponents within the superior longitudinal fascicle in humans: a quantitative, in vivo, DT-MRI study. Cereb Cortex. 2005;15(6):854–69. https://doi.org/10.1093/cercor/bhh186.
3. Petrides M, Pandya DN. Efferent association pathways originating in the caudal prefrontal cortex in the macaque monkey. J Comp Neurol. 2006;498(2):227–51. https://doi.org/10.1002/cne.21048.
4. Catani M, Thiebaut de Schotten M. A diffusion tensor imaging tractography atlas for virtual in vivo dissections. Cortex. 2008;44(8):1105–32. https://doi.org/10.1016/j.cortex.2008.05.004.
5. Rojkova K, Volle E, Urbanski M, Humbert F, Dell'Acqua F. Thiebaut de Schotten M. Atlasing the frontal lobe connections and their variability due to age and education: a spherical deconvolution tractography study. Brain Struct Funct. 2016;221(3):1751–66. https://doi.org/10.1007/s00429-015-1001-3.
6. Thiebaut de Schotten M, Dell'Acqua F, Forkel SJ, et al. A lateralized brain network for visuospatial attention. Nat Neurosci. 2011;14(10):1245–6. https://doi.org/10.1038/nn.2905.
7. Yagmurlu K, Middlebrooks EH, Tanriover N, Rhoton AL Jr. Fiber tracts of the dorsal language stream in the human brain. J Neurosurg. 2016;124(5):1396–405. https://doi.org/10.3171/2015.5.Jns15455.
8. Catani M, Mesulam M. The arcuate fasciculus and the disconnection theme in language and aphasia: history and current state. Cortex. 2008;44(8):953–61. https://doi.org/10.1016/j.cortex.2008.04.002.
9. Mandonnet E, Duffau H. Understanding entangled cerebral networks: a prerequisite for restoring brain function with brain-computer interfaces. Front Syst Neurosci. 2014;8:82. https://doi.org/10.3389/fnsys.2014.00082.
10. Kaplan E, Naeser MA, Martin PI, et al. Horizontal portion of arcuate fasciculus fibers track to pars opercularis, not pars triangularis, in right and left hemispheres: a DTI study. NeuroImage. 2010;52(2):436–44. https://doi.org/10.1016/j.neuroimage.2010.04.247.
11. Doricchi F, Thiebaut de Schotten M, Tomaiuolo F, Bartolomeo P. White matter (dis)connections and gray matter (dys)functions in visual neglect: gaining insights into the brain networks of spatial awareness. Cortex. 2008;44(8):983–95. https://doi.org/10.1016/j.cortex.2008.03.006.
12. Catani M, Mesulam MM, Jakobsen E, et al. A novel frontal pathway underlies verbal fluency in primary progressive aphasia. Brain. 2013;136(Pt 8):2619–28. https://doi.org/10.1093/brain/awt163.
13. Poeppel D, Guillemin A, Thompson J, Fritz J, Bavelier D, Braun AR. Auditory lexical decision, categorical perception, and FM direction discrimination

differentially engage left and right auditory cortex. Neuropsychologia. 2004;42(2):183–200. https://doi.org/10.1016/j.neuropsychologia.2003.07.010.
14. Schmahmann JDPD. Fiber pathways of the brain. Oxford University Press; 2006.
15. Martino J, Brogna C, Robles SG, Vergani F, Duffau H. Anatomic dissection of the inferior fronto-occipital fasciculus revisited in the lights of brain stimulation data. Cortex. 46(5):691–9. https://doi.org/10.1016/j.cortex.2009.07.015.
16. Duffau H. New concepts in surgery of WHO grade II gliomas: functional brain mapping, connectionism and plasticity--a review. J Neuro-Oncol. 2006;79(1):77–115. https://doi.org/10.1007/s11060-005-9109-6.
17. Duffau H, Capelle L, Lopes M, Faillot T, Sichez JP, Fohanno D. The insular lobe: physiopathological and surgical considerations. Neurosurgery. 2000;47(4):801–10.; discussion 810–1. https://doi.org/10.1097/00006123-200010000-00001.
18. Duffau H, Gatignol P, Mandonnet E, Peruzzi P, Tzourio-Mazoyer N, Capelle L. New insights into the anatomo-functional connectivity of the semantic system: a study using cortico-subcortical electrostimulations. Brain. 2005;128(Pt 4):797–810. https://doi.org/10.1093/brain/awh423.
19. Epelbaum S, Pinel P, Gaillard R, et al. Pure alexia as a disconnection syndrome: new diffusion imaging evidence for an old concept. Cortex. 2008;44(8):962–74. https://doi.org/10.1016/j.cortex.2008.05.003.
20. Rudrauf D, Mehta S, Grabowski TJ. Disconnection's renaissance takes shape: formal incorporation in group-level lesion studies. Cortex. 2008;44(8):1084–96. https://doi.org/10.1016/j.cortex.2008.05.005.
21. Moritz-Gasser S, Herbet G, Duffau H. Mapping the connectivity underlying multimodal (verbal and non-verbal) semantic processing: a brain electrostimulation study. Neuropsychologia. 2013;51(10):1814–22. https://doi.org/10.1016/j.neuropsychologia.2013.06.007.
22. Buchsbaum MS, Schoenknecht P, Torosjan Y, et al. Diffusion tensor imaging of frontal lobe white matter tracts in schizophrenia. Ann General Psychiatry. 2006;5:19.
23. Grossi D, Soricelli A, Ponari M, et al. Structural connectivity in a single case of progressive prosopagnosia: the role of the right inferior longitudinal fasciculus. Cortex. 2014;56:111–20. https://doi.org/10.1016/j.cortex.2012.09.010.
24. Beis JM, Keller C, Morin N, et al. Right spatial neglect after left hemisphere stroke: qualitative and quantitative study. Neurology. 2004;63(9):1600–5.
25. Zemmoura I, Herbet G, Moritz-Gasser S, Duffau H. New insights into the neural network mediating reading processes provided by cortico-subcortical electrical mapping. Hum Brain Mapp. 2015;36(6):2215–30. https://doi.org/10.1002/hbm.22766.
26. Fox CJ, Iaria G, Barton JJ. Disconnection in prosopagnosia and face processing. Cortex. 2008;44(8):996–1009. https://doi.org/10.1016/j.cortex.2008.04.003.
27. Ffytche DH. The hodology of hallucinations. Cortex. 2008;44(8):1067–83. https://doi.org/10.1016/j.cortex.2008.04.005.
28. Ross ED. Sensory-specific amnesia and hypoemotionality in humans and monkeys: gateway for developing a hodology of memory. Cortex. 2008;44(8):1010–22. https://doi.org/10.1016/j.cortex.2008.02.002.
29. Koutsarnakis C, Liakos F, Kalyvas AV, Sakas DE, Stranjalis G. A laboratory manual for stepwise cerebral white matter fiber dissection. World Neurosurg. 2015;84(2):483–93. https://doi.org/10.1016/j.wneu.2015.04.018.
30. Gaffan D, Wilson CR. Medial temporal and prefrontal function: recent behavioural disconnection studies in the macaque monkey. Cortex. 2008;44(8):928–35. https://doi.org/10.1016/j.cortex.2008.03.005.
31. Yordanova YN, Duffau H, Herbet G. Neural pathways subserving face-based mentalizing. Brain Struct Funct. 2017;222(7):3087–105. https://doi.org/10.1007/s00429-017-1388-0.
32. Crosby E, Humphrey T, Lauer EW. *White matter of the hemisphere*. Pt 3Correlative anatomy of the nervous system. Macmillan; 1962.
33. Aboitiz F, Montiel J. One hundred million years of interhemispheric communication: the history of the corpus callosum. Braz J Med Biol Res. 2003;36(4):409–20. https://doi.org/10.1590/s0100-879x2003000400002.
34. Witelson SF. Hand and sex differences in the isthmus and genu of the human corpus callosum. A postmortem morphological study. Brain. 1989;112(Pt 3):799–835. https://doi.org/10.1093/brain/112.3.799.
35. Friedrich P, Forkel SJ, Thiebaut de Schotten M. Mapping the principal gradient onto the corpus callosum. NeuroImage. 2020;223:117317.
36. Shah A, Jhawar S, Goel A, Goel A. Corpus callosum and its connections: a finer dissection study. World Neurosurg. 2021;151:e1024–35.
37. Wu Y, Sun D, Wang Y, Wang Y. Subcomponents and connectivity of the inferior Fronto-occipital fasciculus revealed by diffusion Spectrum imaging fiber tracking. Front Neuroanat. 2016;10:88. https://doi.org/10.3389/fnana.2016.00088.
38. Skandalakis GP, Komaitis S, Kalyvas A, et al. Dissecting the default mode network: direct structural evidence on the morphology and axonal connectivity of the fifth component of the cingulum bundle. J Neurosurg. 2020;134(3):1334–45. https://doi.org/10.3171/2020.2.JNS193177.
39. Shah A, Goel A, Jhawar SS, Patil A, Rangnekar R, Goel A. Neural circuitry: architecture and function - a finer dissection study. World Neurosurg. 2019;125:e620–38.
40. Shah A, Jhawar SS, Goel A. Analysis of the anatomy of the Papez circuit and adjoining limbic system by fibre dissection techniques. J Clin Neurosci. 2012;19(2):289–98.